

How flexibility can enhance catalysis

Olivier Rivoire¹

¹*Center for Interdisciplinary Research in Biology (CIRB),
Collège de France, CNRS, INSERM, Université PSL, Paris, France.*

Conformational changes are observed in many enzymes, but their role in catalysis is highly controversial. Here we present a theoretical model that illustrates how rigid catalysts can be fundamentally limited and how a conformational change induced by substrate binding can overcome this limitation, ultimately enabling barrier-free catalysis. The model is deliberately minimal, but the principles it illustrates are general and consistent with many unique features of proteins as well as with previous informal proposals to explain the superiority of enzymes over other classes of catalysts. Implementing the discriminative switch suggested by the model could help overcome limitations currently encountered in the design of artificial catalysts.

Enzymes can accelerate chemical reactions to a level currently unmatched by artificial catalysts from heterogeneous catalysis [1], supramolecular chemistry [2], catalytic antibodies [3] or computational protein design [4]. Could it be that enzymes follow different principles [5–7] or are they simply better [8]? An often-cited difference between enzymes and other catalysts is that enzymes commonly exhibit conformational changes, including along their catalytic cycle [9], while artificial catalysts are generally rigid. Following the principle of transition state stabilization – the cornerstone of catalysis theory – indeed leads to the design of rigid catalysts [3, 4, 10]. On the other hand, the role that flexibility may play in enzyme catalysis is currently very controversial [11–13].

To date, the problem has been studied primarily by experimental and computational studies of model enzymes, with general arguments remaining informal [5–8, 13, 14]. Efforts to develop theoretical physics models mostly date from the 1970s and have left the issue unsettled [15]. Inspired by the power of simple physical models to clarify the mechanisms of protein folding [16] and allostery [17], we use here a minimal model of catalysis to demonstrate in the simplest and clearest terms how catalysis can benefit from flexibility. This approach extends our previous studies of complete catalytic cycles with simple physical models that take into account both geometric and energy constraints [18, 19]. These studies have shown that flexibility is not necessary for catalysis: rigid catalysts can be designed following Pauling’s principle of transition state stabilization [10], which prescribes the geometry, and Sabatier’s principle of intermediate binding energies [20], which prescribes the substrate-catalyst interaction strength.

To explore the design space of catalysts beyond rigid constructs, we reformulate the problem with a lattice model amenable to efficient and exact calculations. This model recapitulates our previous results and further allows us to identify a limit to the extent to which a rigid catalyst can lower activation energies. We then explain how a conformational switch can overcome this limit and enable barrier-free catalysis, with effectively no activation energy. These features are demonstrated for catalyzing bond cleavage in the low-temperature limit or,

equivalently, the limit of high reaction barriers.

Spontaneous reaction – As in our previous works [18, 19], we consider as a spontaneous reaction the dissociation of a dimer into its two constituent monomers but here on a lattice with two particles interacting through a potential $E_s(d_s)$ that is function of their distance d_s in the lattice. The potential excludes two particles from the same site and has two minima, at $d_s = 1$ for the dimer and at $d_s \geq 3$ for the free monomers, with an intermediate transition state at $d_s = 2$. We parametrize this potential by the forward and backward potential barriers, h_s^+ and h_s^- (Fig. 1A). Unless otherwise stated, we take $h_s^+ = 1$ and $h_s^- = 2$.

The locations $x = (x_1, x_2)$ of the two particles define a configuration with associated energy $E(x) = E_s(d_s)$. Each particle can move to a neighboring lattice site with a Metropolis rate $k(x \rightarrow y) = k_0 \min(1, e^{-\beta(E(y) - E(x))})$, where β represents an inverse temperature and k_0 sets the unit of time ($k_0 = 1$ in what follows). The dynamics is thus governed by a master equation with detailed balance. As previously [19], we characterize the spontaneous reaction by the mean first-passage time $T_{S \rightarrow 2P}$ from a configuration S where the particles form a dimer ($d_s = 1$) to a configuration $2P$ where they are free ($d_s \geq 3$; Fig. 1B). For our purposes, the geometry of the lattice is not critical and to permit efficient and exact calculations, we consider a small triangular lattice with $N = 12$ sites (Fig. 1C).

In the low-temperature limit on which we focus, the mean first-passage time $T_{S \rightarrow 2P}$ is controlled by the activation energy $\lim_{\beta \rightarrow \infty} (\ln T_{S \rightarrow 2P}) / \beta = h_s^+$ (Fig. 1D). We write this relation as $T_{S \rightarrow 2P} \sim e^{\beta h_s^+}$ to indicate that pre-factors are negligible when $\beta \rightarrow \infty$. Equivalently, $1/T_{S \rightarrow 2P} \sim e^{-\beta h_s^+}$ corresponds to Arrhenius law.

Rigid catalysis – Following previous works with off-lattice models [18, 19], we first consider a rigid catalyst comprising two binding sites $k = 1, 2$ at distance $L_c = 2$ of each other, which we fix for simplicity at two nodes of the lattice (Fig. 1C). When a particle occupies site k , its energy is lowered by ϵ_{cs}^k where ϵ_{cs}^1 and ϵ_{cs}^2 thus represent the substrate-catalyst interaction energies. The choice $L_c = 2$ is in accordance with Pauling’s principle which prescribes that the geometry of the catalyst should

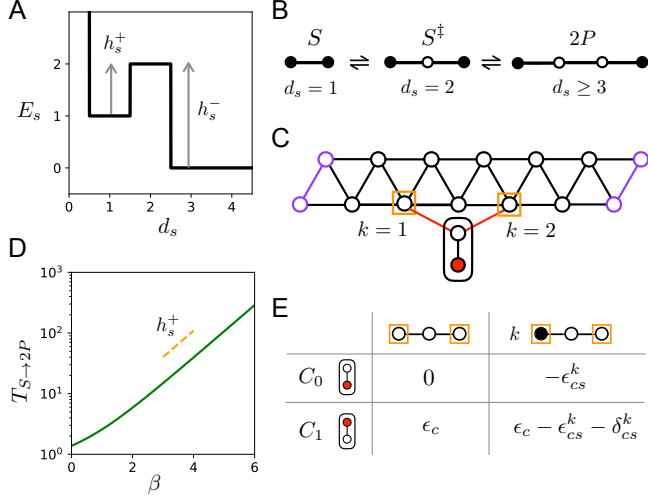


FIG. 1: Model definition – **A**. Potential of interaction between two particles in absence of catalyst, parametrized by the barriers h_s^\pm . **B**. Spontaneous reaction: a dimer S ($d_s = 1$) can dissociate into two particles ($d_s \geq 3$) through passing by a transition state S^\ddagger ($d_s = 2$). **C**. Two-dimensional triangular lattice with 12 nodes and periodic boundary conditions along the horizontal direction (repeated purple nodes). A catalyst is defined by two binding sites ($k = 1, 2$, orange squares) and, if flexible, an internal degree of freedom (red particle confined to the two nodes at the bottom). **D**. Mean first-passage time $T_{S \rightarrow 2P}$, which scales as $T_{S \rightarrow 2P} \sim e^{\beta h_s^+}$ for large values of β . **E**. Interaction energies: in the open state C_0 (red particle down), a substrate particle at site k has a binding energy ϵ_{cs}^k . A flexible catalyst can close to C_1 (red particle up) at an energy cost ϵ_c to provide additional contributions δ_{cs}^k to the binding energies.

be complementary to that of the transition state of the reaction [10].

We characterize the catalyzed reaction by the mean first-passage time $T_{C+S \rightarrow C+2P}$ from initial and configurations where the binding sites are free. The ratio $\eta = T_{S \rightarrow 2P} / T_{C+S \rightarrow C+2P}$ quantifies the efficiency of catalysis with $\eta > 1$ indicating catalysis and $\eta < 1$ inhibition. We find that this catalytic efficiency is symmetric in the interaction energies ϵ_{cs}^1 and ϵ_{cs}^2 (Fig. 2A). As a function of $\epsilon_{cs} = \epsilon_{cs}^1 = \epsilon_{cs}^2$, it exhibits an optimum for $0 < \epsilon_{cs}^* < h_s^+$ (Fig. 2B). As stated by Sabatier’s principle [20] and recurrently observed in heterogeneous catalysis [21], optimal rigid catalysis requires an intermediate binding strength, large enough to lower the activation energy but not too large to allow for efficient product release. As in off-lattice models [18, 19], we also verify that catalysis requires a sufficiently low temperature or, equivalently, a sufficiently large reaction barrier (Fig. 2C).

The efficiency of rigid catalysts is, however, fundamentally limited: when $\beta h_s^+ \gg 1$, they can lower the activation energy by at most a factor two. More precisely, $T_{C+S \rightarrow C+2P} \sim e^{a\beta h_s^+}$ and therefore $\eta \sim e^{(1-a)\beta h_s^+}$ with $a \geq 1/2$ (Fig. 2C-D). This excludes in particular

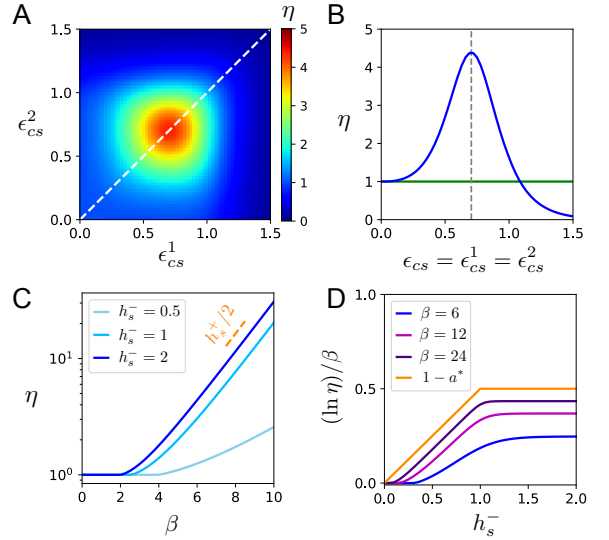


FIG. 2: Rigid catalysis – **A**. Catalytic efficiency $\eta = T_{S \rightarrow 2P} / T_{C+S \rightarrow C+2P}$ of rigid catalysts as a function of the binding strengths ϵ_{cs}^1 and ϵ_{cs}^2 when $\beta = 6$, showing a symmetrical design with $\epsilon_{cs}^1 = \epsilon_{cs}^2$ to be optimal. **B**. Catalytic efficiency for symmetric rigid catalysts, showing a non-trivial optimal binding strength. **C**. Catalytic efficiency of optimal rigid catalysts as a function of the inverse temperature β for different reverse barriers h_s^- , showing that catalysis involves a threshold beyond which the efficiency scales exponentially. **D**. Rescaled catalytic efficiency $(\ln \eta) / \beta$ of optimal rigid catalysts as a function of the reverse barrier h_s^- for different values of β , showing how the bound $\lim_{\beta \rightarrow \infty} (\ln \eta) / \beta \leq 1 - a^*$ implied by Eq. (1) is verified for large β .

barrier-free catalysis defined by $a = 0$, where the catalytic rate does not scale exponentially with temperature anymore, indicating that all activation energies have effectively been annihilated. More precisely, we find (see Supplemental Material)

$$a \geq a^* = \frac{1}{2} + \max\left(0, \frac{h_s^+ - h_s^-}{2h_s^+}\right). \quad (1)$$

This bound can be simply understood in the limit of irreversible reactions ($h_s^- \rightarrow \infty$) when the limiting steps are the transition from a partially to a completely bound complex ($C \cdot S \rightarrow C:S$) and the release of the last product ($C \cdot P + P \rightarrow C + 2P$), which have respectively activation energies $h_s^+ - \epsilon_{cs}$ and ϵ_{cs} . We then have $a \geq \min_{\epsilon_{cs}} \max(h_s^+ - \epsilon_{cs}, \epsilon_{cs}) / h_s^+$, which is achieved for $\epsilon_{cs}^* = h_s^+ / 2$, corresponding to the best trade-off between lowering the activation energy and preventing product sequestration. Eq. (1) also shows that catalysis, which requires $a < 1$, is possible in the $\beta \rightarrow \infty$ limit only if $h_s^- > 0$, i.e., in presence of a reverse barrier.

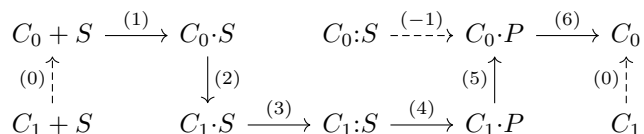
We may wonder if introducing additional binding sites k with non-zero interaction energies ϵ_{cs}^k can improve catalysis. For instance, we may consider the possibility of a third binding site located between the two binding

sites of Figure 1C. Such a three-site catalyst can indeed increase the catalytic efficiency at finite temperature by favoring the correct orientation of the substrate at the expense of a slightly increased activation energy for the chemical transformation. However, this improvement becomes negligible in the $\beta \rightarrow \infty$ limit on which we focus here, where the same bound $a \geq 1/2$ applies: the optimal three-site rigid catalyst is, in fact, the two-site catalyst we have been studying (see Supplementary Material).

Flexible catalysis – An internal degree of freedom to the catalyst can, on the hand other, provide significant improvement without requiring additional binding sites. Here, we assume the catalyst to have two internal states, C_0 (open/inactive) and C_1 (closed/active). Formally, this additional degree of freedom is equivalent to having a third particle confined to two additional lattice sites (Fig. 1C). We parametrize an arbitrary coupling of this internal degree of freedom to the occupancy of the two binding sites by introducing three additional parameters: ϵ_c for the energy of the closed state with respect to the open state and δ_{cs}^k for the additional interaction energies at each bound sites $k = 1, 2$ when in the closed state (Fig. 1E). Rigid catalysts correspond to the limit $\epsilon_c \rightarrow \infty$ that forces the catalyst to remain in a single state.

The presence of an internal degree freedom now allows for barrier-free catalysis, i.e., $T_{C+S \rightarrow C+2P} \sim e^{a\beta h_s^+}$ with $a = 0$. A necessary condition is an energy landscape with a down-hill path from $C + S$ to $C + 2P$ and no kinetic trap, i.e., no local energy minimum besides the final state $C + 2P$. More precisely, since the catalyst can be in two states, we consider such a path between $C_0 + S$ and $C_0 + 2P$ to restore the catalyst in its original state.

For simplicity, let first assume a symmetry between the two binding sites, which reduces the number of parameters to three, ϵ_c , $\epsilon_{cs} = \epsilon_{cs}^1 = \epsilon_{cs}^2 =$ and $\delta_{cs} = \delta_{cs}^1 = \delta_{cs}^2$. Next, consider the following path marked by plain arrows between the different states of the system:



where $C_\sigma + S$ indicates that C is in state σ and not interacting with the substrate, $C_\sigma \cdot S$ that the substrate occupies one binding site, $C_\sigma : S$ that it occupies both, $C_\sigma \cdot P$ that one binding site is occupied by a monomer while the other is free and C_σ that the two binding sites are free and the dimer dissociated. Each step $A \rightarrow B$ involves an activation energy $E_B - E_A$ and requiring no activation energy along the path ($E_B \leq E_A$) implies (1) $0 \leq \epsilon_{cs}$; (2) $\epsilon_c \leq \delta_{cs}$; (3) $h_s^+ \leq \epsilon_{cs} + \delta_{cs}$; (4) $\epsilon_{cs} + \delta_{cs} \leq h_s^-$; (5) $\delta_{cs} \leq \epsilon_c$; (6) $\epsilon_{cs} \leq 0$. In addition, kinetic traps are avoided if the dashed arrows are also associated with negative activation energies, i.e., (-1) $\epsilon_{cs} < h_s^-$, which is implied by (4), and (0) $\epsilon_c > 0$, which is an additional constraint. Assuming $0 < h_s^+ < h_s^-$, these different con-

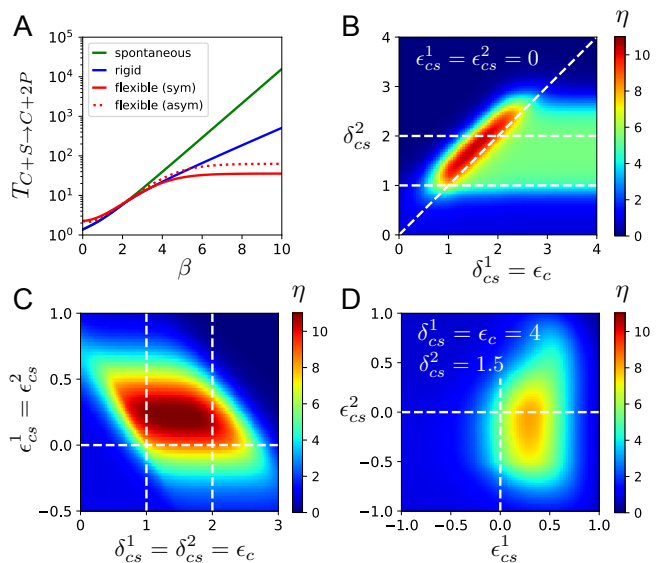


FIG. 3: Flexible catalysis – **A**. Mean first-passage $T_{C+S \rightarrow C+2P}$ from substrate to product in absence of catalyst (green), in presence of an optimal rigid catalyst (blue), a flexible symmetric catalyst with $\epsilon_{cs}^1 = \epsilon_{cs}^2 = 0$ and $\epsilon_c = \delta_{cs}^1 = \delta_{cs}^2 = (h_s^+ + h_s^-)/2 = 1.5$ (full red) or a flexible asymmetric catalyst with $\epsilon_{cs}^1 = \epsilon_{cs}^2 = 0$, $\epsilon_c = \delta_{cs}^1 = 4$ and $\delta_{cs}^2 = 1.5$ (dotted red). $T_{C+S \rightarrow C+2P} \sim e^{a\beta h_s^+}$ for large β where $a = 1$ without catalyst, $a \geq 1/2$ with rigid catalysts but possibly $a = 0$ with flexible catalysts. **B**. Catalytic efficiency $\eta = T_{S \rightarrow 2P} / T_{C+S \rightarrow C+2P}$ as a function of $\delta_{cs}^1 = \epsilon_c$ and δ_{cs}^2 for $\epsilon_{cs}^1 = \epsilon_{cs}^2 = 0$. The horizontal dashed lines delineate the range $h_s^+ < \delta_{cs}^2 < h_s^-$. **C**. Catalytic efficiency for symmetric designs, showing the benefit of a small binding energy $\epsilon_{cs}^1 = \epsilon_{cs}^2 > 0$. **D**. Catalytic efficiency for asymmetric designs with $\epsilon_c = \delta_{cs}^1 = 4$ and $\delta_{cs}^2 = 1.5$ showing the benefit of a small binding energy $\epsilon_{cs}^1 > 0$ at one site only. These benefits arise only at finite β ($\beta = 6$ in B,C,D).

ditions are satisfied simultaneously provided

$$\epsilon_{cs} = 0 \quad \text{and} \quad h_s^+ \leq \delta_{cs} = \epsilon_c \leq h_s^- \quad (2)$$

Taking for instance $\epsilon_c = \delta_{cs} = (h_s^+ + h_s^-)/2$, we verify that $T_{C+S \rightarrow C+2P}$ indeed does not scale exponentially with β any more, the indication of barrier-free catalysis (Fig. 3A).

Alternative designs also leading to barrier-free catalysis are obtained when relaxing the assumption of symmetry between the two binding sites. For instance, a down-hill path where the same site ($k = 1$) is both the first and the last one to be bound is present with no kinetic trap if (see Supplemental Material)

$$\begin{aligned}
 \epsilon_{cs}^1 = 0, \quad \epsilon_{cs}^2 \leq 0, \quad \delta_{cs}^2 \leq \delta_{cs}^1 = \epsilon_c, \\
 \text{and} \quad h_s^+ \leq \epsilon_{cs}^2 + \delta_{cs}^2 \leq h_s^- \quad (3)
 \end{aligned}$$

This requires, as in the symmetric case, an intrinsic energy ϵ_c commensurate with the barrier height, $h_s^+ \leq \epsilon_c$ but, this time, with no upper bound. These condi-

tions are for instance satisfied by taking $\epsilon_{cs}^1 = \epsilon_{cs}^2 = 0$, $\epsilon_c = \delta_{cs}^1 = 2h_s^-$ and $\delta_s^2 = (h_s^- + h_s^+)/2$, again leading to barrier-free catalysis (red dashed curve in Fig. 3A).

At finite temperature, the conditions $\epsilon_{cs}^k = 0$ or $\delta_{cs}^k = \epsilon_c$ should be understood within $\pm 1/\beta$. For example, when $\beta = 6$ as in Figures 3B-D, it is actually optimal for a symmetric catalyst to have $\epsilon_{cs}^1 = \epsilon_{cs}^2 > 0$, which increases the rate at which the substrate induces the open-to-close transition with a tolerable product release penalty (Fig. 3C). For an asymmetric catalyst, only one of the interaction strengths ϵ_{cs}^k benefits from taking a positive value (Fig. 3D).

More generally, three locally optimal designs are numerically found, associated with the two types of designs that we identified in the $\beta \rightarrow \infty$ limit: a symmetric design with $\epsilon_{cs}^1 = \epsilon_{cs}^2 > 0$ and $h_s^+ < \epsilon_c = \delta_{cs}^1 = \delta_{cs}^2 < h_s^-$ and two asymmetric designs related by the $1 \leftrightarrow 2$ symmetry with respectively $\delta_{cs}^1 \ll \delta_{cs}^2 = \epsilon_c$ and $\delta_{cs}^2 \ll \delta_{cs}^1 = \epsilon_c$ (see Supplemental Material). The symmetric design is the global optimum, but its catalytic efficiency is no more than twice that of the asymmetric designs.

Discussion – Based on the formulation and solution of an elementary model of catalysis, we have illustrated how the presence of a degree of freedom internal to the catalyst can overcome the limitations of rigid catalysis and effectively enable the annihilation of all activation energies. The same limitations of rigid catalysts are also observed in off-lattice models [19]. They arise from the antagonistic effect of binding energies which, with rigid catalysts, cannot lower activation energies without sequestering the products. This effect is widely observed in heterogeneous catalysis, where it takes the form of volcano-shaped plots [22] comparable to Figure 2B. The mechanism by which the conflict is resolved in our model is also general, and relies on the capacity of conformational switches to confer high specificity [23], here to the transition state of the reaction.

Although, to our knowledge, this mechanism of catalysis through a discriminative switch has not been formalized before, it echoes multiple empirical observations and informal hypotheses made in enzymology. Koshland long-ago pointed out that conformational changes induced by ligand binding are essential to enzymes [24], advocating an “induced-fit theory” to replace Fischer’s “lock-and-key theory” that views enzymes as rigid bodies [25]. His theory, however, concerns substrate and not transition-state specificity. For the later, Jencks stressed the role of an “intrinsic binding energy” much greater than the observed binding energy [5], which corresponds in our model to $\epsilon_{cs} \ll \delta_{cs}$. Our model also substantiates the hypothesis that enzymes can act as molecular machines [26]. Finally, closer to our results is the interpretation given by Richard of the presence of a conformational switch in several of the most efficient enzymes [14]. Our model formalizes these previous insights and conforms with the extensive data on which they are based without contradicting either the experimental observations of conformational fluctuations occurring on the time scale

of enzymatic reactions, as revealed both by NMR and single-molecule experiments [27, 28], nor the many indications that flexibility plays no significant role for the chemical transformation itself [29, 30]. The role of the switch in our model is indeed not to accelerate this step but to make its acceleration compatible with the completion of other steps of the catalytic cycle. In fact, we previously found that introducing flexibility along the reaction coordinate can be detrimental for catalysis [18, 19].

Still, the merits of a discriminative switch do not preclude additional benefits from enzyme flexibility, whether to optimize local environments through substrate encapsulation [31] or to enable allosteric regulation, although in this latter case a more parsimonious explanation is that a switch first evolved for transition-state discrimination before its recruitment for regulation [23, 32]. Flexibility may also provide additional benefits when multiple transition states have to be crossed [33].

Of the two types of design that can achieve barrier-free catalysis in our model, the asymmetric design seems more relevant for enzymes, which typically have asymmetric substrates and distinct active and binding sites. This design is remarkable from an evolutionary standpoint as it does not require any specific energy tuning – in contrast with rigid catalysts. The constraint $\delta_{cs}^1 = \epsilon_c$ is indeed independent of the reaction parameters h_s^\pm , and δ_{cs}^1 only needs to be large enough while δ_{cs}^2 can take any value in the range $[h_s^+, h_s^-]$ (Fig. 3B).

Finally, our model exemplifies how a conformational switch can enable barrier-free catalysis but does not account for the limited binding energy that individual atoms can effectively provide. In enzymes, the large free energy compensation upon switching (of ϵ_c by δ_c^1) must therefore involve atoms of substrates beyond those chemically transformed, consistent with the otherwise puzzling implication of non-reactive parts of substrates that Jencks viewed as the essential difference between enzymatic and non-enzymatic catalysis [5]. Furthermore, the unfavorable modification induced by ligand binding (with cost ϵ_c) may take different forms in enzymes, e.g., entropic changes or non-mechanical strains, as well as involve the substrate itself as what primarily matters is a free-energy difference between two states of the substrate-catalyst complex.

Finally, not all enzymes need to work by the same mechanism. For instance, some of the less efficient enzymes may act more like rigid catalysts [6]. Moreover, our optimal flexible catalyst enables barrier-free catalysis but, like most enzymes, is subject to futile encounters [34], while diffusion-limited enzymes are also known that are limited only by the enzyme-substrate collision rate [35]. The purpose of our model, however, is not to account for the diversity of enzyme activities but to demonstrate how a discriminating switch can, at least in one well-defined case, enhance catalysis, thus providing a new basis for studying the role of flexibility in understanding natural enzymes and designing artificial catalysts.

Acknowledgments – I am grateful to C. Nizak, M. Muñoz Basagoiti, Y. Sakref, Z. Zeravcic and I. Junier

for discussions, and to ANR-21-CE45-0033 for funding.

-
- [1] J Greeley. Theoretical Heterogeneous Catalysis: Scaling Relationships and Computational Catalyst Design. *Annual Review of Chemical and Biomolecular Engineering*, 7(1):1–31, 2015.
- [2] J K M Sanders. Supramolecular Catalysis in Transition. *Chemistry ? A European Journal*, 4(8):1378–1383, 1998.
- [3] D S Tawfik, Zelig E, and B S Green. Catalytic antibodies: A critical assessment. *Molecular Biotechnology*, 1(1):87–103, 1994.
- [4] S L Lovelock, R Crawshaw, S Basler, C Levy, D Baker, D Hilvert, and A P Green. The road to fully programmable protein catalysis. *Nature*, 606(7912):49–58, 2022.
- [5] W P Jencks. Advances in Enzymology and Related Areas of Molecular Biology. *Advances in Enzymology - and Related Areas of Molecular Biology*, 43:219–410, 1975.
- [6] A J Kirby, F Hollfelder, and D S Tawfik. Nonspecific catalysis by protein surfaces. *Applied Biochemistry and Biotechnology*, 83(1-3):173–181, 2000.
- [7] G Swiegers. *Mechanical catalysis: methods of enzymatic, homogeneous, and heterogeneous catalysis*. John Wiley & Sons, 2008.
- [8] J R Knowles. Enzyme catalysis: not different, just better. *Nature*, 350(6314):121–124, 1991.
- [9] K A Henzler-Wildman, V Thai, M Lei, M Ott, M Wolf-Watz, T Fenn, E Pozharski, M A Wilson, G A Petsko, M Karplus, C G Hubner, and D Kern. Intrinsic motions along an enzymatic reaction trajectory. *Nature*, 450(7171):838–844, 2007.
- [10] L Pauling. Molecular architecture and biological reactions. *Chemical and engineering news*, 00 1946.
- [11] S C L Kamerlin and A Warshel. At the dawn of the 21st century: Is dynamics the missing link for understanding enzyme catalysis? *Proteins: Structure, Function, and Bioinformatics*, 78(6):1339–1375, 2010.
- [12] A Kohen. Role of Dynamics in Enzyme Catalysis: Substantial versus Semantic Controversies. *Accounts of Chemical Research*, 48(2):466–473, 2015.
- [13] P K Agarwal. A Biophysical Perspective on Enzyme Catalysis. *Biochemistry*, 58(6):438–449, 2019.
- [14] J P Richard. Protein Flexibility and Stiffness Enable Efficient Enzymatic Catalysis. *Journal of the American Chemical Society*, 141(8):3320–3331, 2019.
- [15] G R Welch, B Somogyi, and S Damjanovich. The role of protein fluctuations in enzyme action: A review. *Progress in Biophysics and Molecular Biology*, 39(2):109–146, 1982.
- [16] V S Pande, A Y Grosberg, and T Tanaka. Statistical mechanics of simple models of protein folding and design. *Biophysical journal*, 73(6):3192 – 3210, 12 1997.
- [17] E Rouviere, R Ranganathan, and O Rivoire. On the emergence of single versus multi-state allostery. *arXiv preprint arXiv:2111.09377*, 2021.
- [18] O Rivoire. Geometry and Flexibility of Optimal Catalysts in a Minimal Elastic Model. *The journal of physical chemistry. B*, 124(5):807 – 813, 02 2020.
- [19] M Muñoz-Basagoiti, O Rivoire, and Z Zeravcic. Catalysis from the bottom-up. *arXiv preprint arXiv:2211.12107*, 2022.
- [20] P Sabatier. *La catalyse en chimie organique*. Libraire Polytechnique, 1913.
- [21] A J Medford, A Vojvodic, and J S Hummelshoj. From the Sabatier principle to a predictive theory of transition-metal heterogeneous catalysis. *Journal of Catalysis*, 328:36 – 42, 00 2015.
- [22] T Bligaard, J K Norskov, S Dahl, J Matthiesen, C H Christensen, and J Sehested. The Bronsted-Evans-Polanyi relation and the volcano curve in heterogeneous catalysis. *Journal of Catalysis*, 224(1):206–217, 2004.
- [23] O Rivoire. Parsimonious evolutionary scenario for the origin of allostery and coevolution patterns in proteins. *Physical Review E*, 100(3-1):032411, 09 2019.
- [24] D E Koshland. Application of a Theory of Enzyme Specificity to Protein Synthesis. *Proceedings of the National Academy of Sciences*, 44(2):98 – 104, 02 1958.
- [25] E Fischer. Einfluss der configuration auf die wirkung der enzyme. *Berichte der deutschen chemischen Gesellschaft*, 27(3):2985–2993, 1894.
- [26] H F Fisher and N Singh. Transduction of enzyme?ligand binding energy into catalytic driving force. *FEBS Letters*, 294(1-2):1–5, 1991.
- [27] H Yang, G Luo, P Karnchanaphanurach, T-M Louie, I Rech, S Cova, L Xun, and X S Xie. Protein conformational dynamics probed by single-molecule electron transfer. *Science*, 302(5643):262–266, 2003.
- [28] E Z Eisenmesser, O Millet, W Labeikovsky, D M Korzhnev, M Wolf-Watz, D A Bosco, J J Skalicky, L E Kay, and D Kern. Intrinsic dynamics of an enzyme underlies catalysis. *Nature*, 438(7064):117–121, 2005.
- [29] I Tunon, D Laage, and J T Hynes. Are there dynamical effects in enzyme catalysis? Some thoughts concerning the enzymatic chemical step. *Archives of Biochemistry and Biophysics*, 582:42–55, 2015.
- [30] A Warshel and R P Bora. Perspective: Defining and quantifying the role of dynamics in enzyme catalysis. *The Journal of Chemical Physics*, 144(18):180901, 05 2016.
- [31] J P Richard, T L Amyes, B Goryanova, and X Zhai. Enzyme architecture: on the importance of being in a protein cage. *Current Opinion in Chemical Biology*, 21:1–10, 2014.
- [32] S M Coyle, J Flores, and W A Lim. Exploitation of latent allostery enables the evolution of new modes of MAP kinase regulation. *Cell*, 154(4):875 – 887, 08 2013.
- [33] J Kraut. How do enzymes work? *Science*, 242(4878):533 – 540, 10 1988.
- [34] A Bar-Even, R Milo, E Noor, and D S Tawfik. The Moderately Efficient Enzyme: Futile Encounters and Enzyme Floppiness. *Biochemistry*, 54(32):4969 – 4977, 08 2015.
- [35] J R Knowles and W J Albery. Perfection in enzyme catalysis: the energetics of triosephosphate isomerase. *Accounts of Chemical Research*, 10(4):105–111, 1977.

Supplemental Material

Model definition

A configuration $x = (x_1, x_2, \sigma_c)$ of the system consists of the locations x_1, x_2 of the two particles on the lattice together with the state σ_c of the catalyst, which may be open ($\sigma_c = 0$) or closed ($\sigma_c = 1$). We denote by $d_s = d(x_1, x_2)$ the distance between the particles, defined by the length of the shortest connecting path on the lattice, and by $\sigma_k = 1$ the occupancy of binding site k , with $\sigma_k = 0$ indicating that it is vacant ($k = 1, 2$). In terms of these variables, the energy of configuration x is

$$E(x) = E_s(d_s) + E_c(\sigma_c) - \sum_{k=1,2} E_{cs}^k(\sigma_c) \sigma_k \quad (\text{S1})$$

where

$$E_s(d_s) = \begin{cases} +\infty & \text{if } d_s = 0 \\ h_s^- - h_s^+ & \text{if } d_s = 1 \\ h_s^- & \text{if } d_s = 2 \\ 0 & \text{if } d_s \geq 3 \end{cases} \quad (\text{S2})$$

as represented in Fig. 1A,

$$E_c(\sigma_c) = \epsilon_c \sigma_c \quad (\text{S3})$$

and

$$E_{cs}^k(\sigma_c) = \epsilon_{cs}^k + \delta_{cs}^k \sigma_c \quad (\text{S4})$$

as represented in Fig. 1D. The spontaneous reaction corresponds to $\epsilon_{cs}^k = 0$ and rigid catalysts to $\epsilon_c = \infty$.

The system can transition from $x = (x_1, x_2, \sigma_c)$ to any of the configurations y given by (y_1, x_2, σ_c) , (x_1, y_2, σ_c) , $(x_1, x_2, 1 - \sigma_c)$ where $d(x_1, y_1) = 1$ and $d(x_2, y_2) = 1$. These transitions occur with Metropolis rates given by

$$k(x \rightarrow y) = k_0 \min(1, e^{-\beta(E(y) - E(x))}). \quad (\text{S5})$$

where $k_0 = 1$ sets the unit of time. This defines a master equation with detailed balance in the form of a continuous-time discrete Markov process,

$$\partial_t \pi(x, t) = \sum_{y \neq x} (\pi(y, t) k(y \rightarrow x) - \pi(x, t) k(x \rightarrow y)) \quad (\text{S6})$$

where $\pi(x, t)$ is the probability to be in configuration x at time t . The generalization to more than two binding sites is straightforward.

Mean first-passage times

For the spontaneous reaction, we define S as the set of configurations with $d_s = 1$ and $2P$ as the set of configurations with $d_s \geq 3$. With $T_{x \rightarrow 2P}$ denoting the mean

first-passage time from $x \in S$ to $2P$, we define the global mean first-passage time $T_{S \rightarrow 2P}$ by

$$T_{S \rightarrow 2P} = \frac{1}{|S|} \sum_{x \in S} T_{x \rightarrow 2P} \quad (\text{S7})$$

where $|S|$ is the size of set S .

For the catalyzed reaction, we define $C+S$ as the set of configurations with $d_s = 1$ and $\sigma_1 = \sigma_2 = 0$, and $C+2P$ as the set of configurations with $d_s \geq 3$ and $\sigma_1 = \sigma_2 = 0$. We define $T_{C+S \rightarrow C+2P}$ as

$$T_{C+S \rightarrow C+2P} = \frac{1}{|C+S|} \sum_{x \in C+S} T_{x \rightarrow C+2P}. \quad (\text{S8})$$

We compute mean first-passage times exactly by linear algebra. In general, given $Q_{xy} = k(x \rightarrow y)$ for $x \neq y$ and $Q_{xx} = -\sum_{y \neq x} k(x \rightarrow y)$, the mean first-passage time $T_{y \rightarrow B}$ from a configuration $y \notin B$ to a set B is solution of the equations $\sum_{x \notin B} Q_{xy} T_{y \rightarrow B} = -1$ [1]. Introducing \tilde{Q} defined over configurations not in B by $\tilde{Q}_{xy} = Q_{xy}$, this corresponds to solving the matrix equation $\tilde{Q} T_{\rightarrow B} = -U$ where U is a vector whose components are all one. In practice, the matrix \tilde{Q} may be ill-conditioned, which prevents the application of this method to arbitrary large values of β .

Activation energy for the spontaneous reaction

In the low-temperature limit $\beta \rightarrow \infty$ on which we focus, we can ignore the contribution of diffusional processes and estimate $T_{S \rightarrow 2P}$ as the mean first-passage time from S to $2P$ for the Markov chain

$$S \xrightleftharpoons[\rho_{-1}]{\rho_1} S^\ddagger \xrightarrow{\rho_2} 2P \quad (\text{S9})$$

with, since $h_s^+ > 0$ and $h_s^- > 0$,

$$\rho_1 \sim e^{-\beta h_s^+}, \quad \rho_{-1} \sim 1, \quad \rho_2 \sim 1 \quad (\text{S10})$$

where the pre-factors play no role in the $\beta \rightarrow \infty$ limit. The mean first-passage time is

$$T_{S \rightarrow 2P} = \frac{1}{\rho_1} + \frac{1}{\rho_2} + \frac{\rho_{-1}}{\rho_1 \rho_2}. \quad (\text{S11})$$

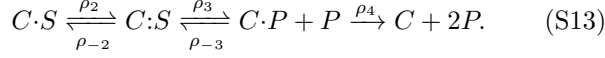
which leads to

$$\lim_{\beta \rightarrow \infty} \frac{1}{\beta} \ln T_{S \rightarrow 2P} = h_s^+. \quad (\text{S12})$$

Activation energy for two-site rigid catalysts

We analyze here the symmetric case $\epsilon_{cs}^1 = \epsilon_{cs}^2 = \epsilon_{cs}$ which Fig. 2 shows to include the optimal designs. As for the spontaneous reaction, the problem reduces in the $\beta \rightarrow \infty$ limit to a Markov chain where diffusion is neglected. Here, the relevant states are, in addition to $C+S$ and $C+2P$, state $C\cdot S$ defined by $d_s = 1$ and $\sigma_1 + \sigma_2 = 1$, state $C:S$ defined by $d_s = 2$ and $\sigma_1 + \sigma_2 = 2$ and state $C\cdot P + P$ defined by $d_s \geq 3$ and $\sigma_1 + \sigma_2 = 1$.

To obtain a lower bound on $T_{C+S \rightarrow C+2P}$, we can start from $C\cdot S$ and consider



to which is associated the mean first-passage time

$$T_{C\cdot S \rightarrow C+2P} = \frac{1}{\rho_2} + \frac{1}{\rho_3} + \frac{1}{\rho_4} + \frac{\rho-2}{\rho_2\rho_3} + \frac{\rho-3}{\rho_3\rho_4} + \frac{\rho-2\rho-3}{\rho_2\rho_3\rho_4} \quad (\text{S14})$$

If $\epsilon_{cs} > h_s^+$, then $1/\rho_4 \sim e^{\beta\epsilon_{cs}}$ cannot be lower than $T_{S \rightarrow 2P}$. We therefore consider $\epsilon_{cs} < h_s^+$. Next, if $\epsilon_{cs} > h_s^-$, $\rho-2\rho-3/(\rho_2\rho_3\rho_4) \sim e^{\beta(h_s^+ - h_s^- + \epsilon_{cs})}$ cannot be lower than $T_{S \rightarrow 2P}$. We therefore also consider $\epsilon_{cs} < h_s^-$. Under these conditions we have

$$\begin{aligned} \rho_2 &\sim e^{-\beta(h_s^+ - \epsilon_{cs})}, & \rho-2 &\sim 1, & \rho_3 &\sim 1 \\ \rho-3 &\sim e^{-\beta(h_s^- - \epsilon_{cs})}, & \rho_4 &\sim e^{-\beta\epsilon_{cs}}. \end{aligned} \quad (\text{S15})$$

It follows that h_c^+ defined by

$$h_c^+ = \lim_{\beta \rightarrow \infty} \frac{1}{\beta} \ln T_{C\cdot S \rightarrow C+2P} \quad (\text{S16})$$

is given by

$$h_c^+ = \max(h_s^+ - \epsilon_{cs}, \epsilon_{cs}, 2\epsilon_{cs} - h_s^-, h_s^+ - h_s^- + \epsilon_{cs}). \quad (\text{S17})$$

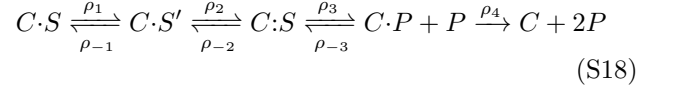
Optimal rigid catalysts have activation energy $\min_{\epsilon_{cs}} h_c^+(\epsilon_{cs})$. In the limit $h_s^- \rightarrow \infty$ of irreversible reactions where $h_c^+(\epsilon_{cs}) = \max(h_s^+ - \epsilon_{cs}, \epsilon_{cs})$ the optimum over ϵ_{cs} is obtained for $h_s^+ - \epsilon_{cs} = \epsilon_{cs}$, leading to $\epsilon_{cs}^* = h_s^+/2$ and $h_c^+(\epsilon_{cs}^*) = h_s^+/2$. This expression is valid as long as no other term in Eq. (S17) exceeds $h_s^+/2$ when considering $\epsilon_{cs} = \epsilon_{cs}^*$. The largest value of h_s^- at which this ceases to be the case is $h_s^- = h_s^+$ due to the term $h_s^+ - h_s^- + \epsilon_{cs}$. For $h_s^- < h_s^+$, this term dominates over ϵ_{cs} and the optimum is obtained when $h_s^+ - \epsilon_{cs} = h_s^+ - h_s^- + \epsilon_{cs}$, leading to $\epsilon_{cs}^* = h_s^-/2$ and $h_c^+(\epsilon_{cs}^*) = h_s^+ - h_s^-/2$. Finally, $a^* = \min_{\epsilon_{cs}} h_c^+(\epsilon_{cs})/h_s^+$ is therefore given by Eq. (1).

Three-site rigid catalysts

The model can be extended to consider a third binding site $k = 3$ located between the two binding sites $k = 1$ and $k = 2$ of Fig. 1C. Optimizing $T_{C+S \rightarrow C+2P}$ over the

three parameters $\epsilon_{cs}^1, \epsilon_{cs}^2, \epsilon_{cs}^3$ leads again to an optimum that is symmetric with respect to $1 \leftrightarrow 2$. While the optimum involves $\epsilon_{cs}^3 > 0$ at finite β , it requires $\epsilon_{cs}^3 = 0$ when $\beta \rightarrow \infty$, which corresponds to the two-site catalyst considered in the main text. The bound $a \geq 1/2$ therefore applies even when considering a third binding site $k = 3$ located between $k = 1$ and $k = 2$.

This can be demonstrated by following the same reasoning as for two-site catalysts, first reducing the problem to two parameters $\epsilon_{cs} = \epsilon_{cs}^1 = \epsilon_{cs}^2$ and $\epsilon'_{cs} = \epsilon_{cs}^3$ by assuming the symmetry $1 \leftrightarrow 2$ and then considering the coarse-grained Markov chain



where $C\cdot S'$ denotes the configurations $d_s = 1$ with the third site being occupied in addition to one of the sites $k = 1, 2$, and where $C:S$ exclude these configurations. Let $h_c^+(\epsilon_{cs}, \epsilon'_{cs}) = \lim_{\beta \rightarrow \infty} \ln(T_{C\cdot S \rightarrow C+2P})/\beta$ and let consider the most favorable case of irreversible reactions with $h_s^- = \infty$. As shown above, we have then $h_c^+(\epsilon_{cs}, 0) = \max(h_s^+ - \epsilon_{cs}, \epsilon_{cs})$. If $\epsilon'_{cs} > 0$, this becomes $h_c^+(\epsilon_{cs}, \epsilon'_{cs}) = \max(h_s^+ - \epsilon_{cs} + \epsilon'_{cs}, \epsilon_{cs}) \geq h_c^+(\epsilon_{cs}, 0)$. When $\beta \rightarrow \infty$ no benefit is therefore obtained from considering $\epsilon'_{cs} > 0$.

If instead $\epsilon'_{cs} < 0$, we have $\rho_1 \sim e^{\beta\epsilon'_{cs}}$, $\rho-1 \sim 1$, $\rho_2 \sim e^{-\beta(h_s^+ - \epsilon_{cs} + \epsilon'_{cs})}$, $\rho_4 \sim e^{-\beta\epsilon_{cs}}$ and from

$$T_{C\cdot S' \rightarrow C+2P} \geq \frac{\rho-1}{\rho_1\rho_2} + \frac{1}{\rho_4} \quad (\text{S19})$$

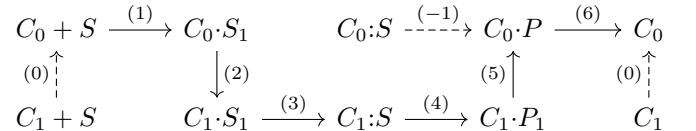
we get

$$h_c^+(\epsilon_{cs}, \epsilon'_{cs}) \geq \max(h_s^+ - \epsilon_{cs}, \epsilon_{cs}) = h_c^+(\epsilon_{cs}, 0) \quad (\text{S20})$$

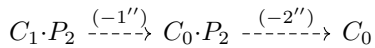
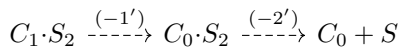
so that, when $\beta \rightarrow \infty$, no benefit is obtained from considering $\epsilon'_{cs} < 0$. The optimal three-site catalyst is therefore a two-site catalyst with $\epsilon'_{cs} = 0$.

Asymmetric two-state catalysts

We indicate by $C_{\sigma_c} \cdot S_k$ and $C_{\sigma_c} \cdot P_k$ that a catalyst in state σ_c is bound to a single particle of the substrate at site k and consider the following down-hill path:



to which we add the following down-hill paths to prevent kinetic traps:



The requirements for each of the arrow to be down-hill are (1) $0 \leq \epsilon_{cs}^1$, (2) $\epsilon_c \leq \delta_{cs}^1$, (3) $h_s^+ \leq \epsilon_{cs}^2 + \delta_{cs}^2$, (4) $\epsilon_{cs}^2 + \delta_{cs}^2 \leq h_s^-$, (5) $\delta_{cs}^1 \leq \epsilon_c$, (6) $\epsilon_{cs}^1 \leq 0$, $(-1')$ and $(-1'')$ $\delta_{cs}^2 \leq \epsilon_c$, $(-2')$ and $(-2'')$ $\epsilon_{cs}^2 \leq 0$, which lead to the conditions summarized in Eq. (3).

Numerical optimization

For $\beta = 6$, maximizing numerically the catalytic efficiency η over the parameters $\epsilon_{cs}^1, \epsilon_{cs}^2, \delta_{cs}^1, \delta_{cs}^2, \epsilon_c$ by gra-

dient descent using the function `optimize` with option `GradientDescent()` from the Julia package `Optim.jl` [2] leads to (at least) three different local minima, depending on the initial conditions:

A symmetric optimum with $\epsilon_{cs}^1 \simeq \epsilon_{cs}^2 \simeq 0.14$, $\delta_{cs}^1 = \delta_{cs}^2 \simeq 1.47$, $\epsilon_c \simeq 1.35$ when starting from $(\epsilon_{cs}^1, \epsilon_{cs}^2, \epsilon_c, \delta_{cs}^1, \delta_{cs}^2) = (0.2, 0.2, 1.5, 1.5, 1.5)$.

Two asymmetric optima related by $1 \leftrightarrow 2$ symmetry with $\epsilon_{cs}^1 \simeq 0.21$, $\epsilon_{cs}^2 \simeq -0.09$, $\delta_{cs}^1 \simeq 3.01$, $\delta_{cs}^2 \simeq 1.66$, $\epsilon_c \simeq 2.90$ when starting from $(\epsilon_{cs}^1, \epsilon_{cs}^2, \epsilon_c, \delta_{cs}^1, \delta_{cs}^2) = (0.1, -0.1, 3., 3., 1.5)$.

The symmetric optimum is $1.4\times$ more efficient than the asymmetric one.

-
- [1] S Iyer-Biswas and A Zilman. First-passage processes in cellular biology. *Advances in chemical physics*, 160:261–306, 2016.
- [2] P K Mogensen and A N Riseth. Optim: A mathematical optimization package for Julia. *Journal of Open Source Software*, 3(24):615, 2018.